





cambridge.org/mrf

Thomas Uguen^{1,2} , Raphael Gillard¹, Renaud Loison¹ ,
Jeanne Pages-Mounic² and Philippe Pouliguen³

¹Univ. Rennes, INSA Rennes, CNRS, IETR-UMR 6164, Rennes 35000, France; ²CNES, 18 Avenue Edouard Belin, Toulouse 31400, France and ³DGA-AID, 60 Bd. du général Martial Valin, Paris 75509, France

Research Paper

Cite this article: Uguen T, Gillard R, Loison R, Pages-Mounic J, Pouliguen P (2024) On the use of autocorrelation properties for diffuse reflection by coding metasurfaces. *International Journal of Microwave and Wireless Technologies*, 1–7. <https://doi.org/10.1017/S1759078724001168>

Received: 28 June 2024
Revised: 4 October 2024
Accepted: 15 October 2024

Keywords:

coding metasurface; diffuse scattering; RCS reduction

Corresponding author: Thomas Uguen;
Email: Thomas.Uguen@insa-rennes.fr

Abstract

One-bit coding metasurfaces combine two basic unit cells with out-of-phase responses. Their potential in achieving diffuse scattering has already been demonstrated. These metasurfaces can subsequently be applied to radar-signature control. This paper presents a theoretical analysis linking the scattered field to the autocorrelation of the code that encodes the metasurface. This analysis leads to a focus on Minimum Peak Sidelobes codes with autocorrelation characteristics similar to the unit impulse. Advances in other research areas have greatly enhanced the search for these kind of codes, making them directly usable for coding diffuse scattering metasurfaces. This approach is compared with existing codes, specifically examining how it performs against the optimal code found through exhaustive search in small-scale scenarios. Then, it is shown that this coding strategy facilitates the design of metasurfaces with any and large electrical sizes, achieving results comparable to those obtained through optimization-based approaches, at a significantly reduced computational workload.

Introduction

Over the past decade, metasurfaces have revolutionized electromagnetic (EM) wavefront manipulation, enabling a diverse range of applications. In the field of radar, their capabilities extend to areas such as anomalous reflection [1, 2], backscattering enhancement [3], and radar cross-section reduction (RCSR) [4, 5]. Diffuse scattering metasurfaces represent a promising technique for bistatic RCSR [6].

The present study focuses specifically on the concept of coding metasurfaces, which leverage a limited number of unit-cells represented by a binary code [7]. In the simplest implementation, only two different elements, labeled as “1” and “0”, are used. Therefore, the metasurface is represented as a 2D binary matrix. By arranging these elements in specific patterns, the scattering fields can be manipulated to achieve various functionalities [8]. The idea behind coding diffuse scattering metasurfaces is to achieve uniform scattering of an incident EM wave in all directions. Thus, the primary goal when designing such a metasurface is to determine the optimal arrangement of binary elements within the coding matrix to achieve the best diffusion.

Various approaches are present in the literature such as the checkerboard configuration [4, 5]. By arranging binary elements in a chessboard pattern, the incident EM wave is reflected into four main directions and the radar cross-section (RCS) is minimized in the specular direction. Another strategy involves randomly distributing the elements within the matrix to try to maximize destructive interferences and thus decrease the bistatic RCS [9, 10]. These initial two approaches are directly applicable and do not require computation time for synthesis. However, their performance is limited as the diffusion is not optimal. Another approach could be optimization [11, 12]. This method allows for good scattering performance but is highly costly in terms of time and computational resources. Finally, a method based on Golay–Rudin–Shapiro polynomials, which lead to Golay codes, allows for the fast synthesis of coded diffuse scattering metasurfaces [6]. That analytical method does not require extensive computational costs and it is applicable for codes of size 2^i , where i is a natural number. This enables the suboptimal encoding of large-sized metasurfaces. Such a method is regarded as the most advantageous solution in terms of time versus performance trade-off for encoding a diffuse scattering metasurface. However, the constraint to use a code whose length is 2^i lacks flexibility.

In this context, a new coding strategy based on Minimum Peak Sidelobes (MPS) codes is introduced in this paper. These codes, used in other fields, are valuable for encoding metasurfaces for RCSR. This work also provides a detailed assessment of the different codes from the literature, including the newly introduced ones.

© The Author(s), 2024. Published by Cambridge University Press in association with The European Microwave Association. This is an Open Access article, distributed under the terms of the Creative Commons Attribution licence (<http://creativecommons.org/licenses/by/4.0>), which permits unrestricted re-use, distribution and reproduction, provided the original article is properly cited.

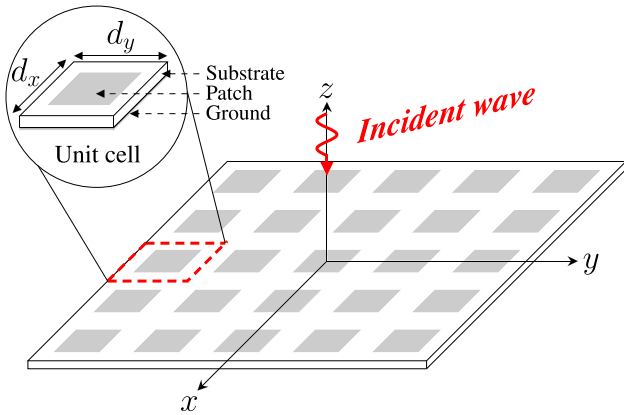


Figure 1. General printed metasurface configuration.

Section “Background theory and modeling” presents the theory and modeling of metasurfaces, with a particular focus on the concept of coding metasurfaces. The link between the metasurface radiation and the autocorrelation of the code is also discussed, leading to design rules for selecting this code. Section “1D coding metasurfaces for diffuse scattering” provides a detailed analysis of 1D coding metasurfaces for diffuse scattering, including an exhaustive search for optimal codes that achieve low directivity. It also compares the performance of established codes from the literature with the MPS codes introduced in this paper, relative to the optimal solutions. Section “Design examples” provides design examples of large 1D metasurfaces. Then, the classical dyadic product is used to extend the 1D codes to 2D metasurfaces.

Background theory and modeling

Metasurface configuration

A metasurface is a 2D panel composed of $M \times N$ unit-cells. Each unit-cell is characterized by a complex reflection coefficient with amplitude Γ_{mn} and phase φ_{mn} . The periodicities of the metasurface along the x and y axes are denoted as d_x and d_y , respectively. An example of a metasurface in printed technology with patches as unit-cells is shown in Figure 1.

A widely used configuration in the literature is the 1-bit coding metasurface involving only two different possible phase states. All the results in this article are based on this concept. As illustrated in Figure 2, a particular metasurface with two phase states, denoted as φ_1 and φ_2 , where the phase difference is $\Delta\varphi = |\varphi_1 - \varphi_2| = \pi$, can be represented by a coding matrix. In this representation, φ_1 corresponds to the binary element 0, and φ_2 corresponds to the binary element 1. Thus, the phase responses of the 0 and 1 elements

are simply defined as $\varphi_n = n\pi$ rad ($n = 0, 1$). A common example of cells that meet these conditions are the artificial magnetic conductor and perfect electric conductor cells [4].

Analytical modeling

To quickly and efficiently compute the scattered field E_s of a metasurface, the simple antenna array theory is used [13]. The field reflected by the metasurface when illuminated by an incident plane wave is defined by equation (1), where $f(\theta, \phi)$ represents the radiation of the unit-cells, E_0 is the magnitude of the incident wave, and α_{mn} its phase on the unit-cell (m, n)

$$E_s(\theta, \phi) = \sum_{m=0}^{M-1} \sum_{n=0}^{N-1} E_0 e^{j\alpha_{mn}} \cdot \Gamma_{mn} e^{j\varphi_{mn}} \cdot f(\theta, \phi) \cdot e^{jk(md_x \sin \theta \cos \phi + nd_y \sin \theta \sin \phi)} \tag{1}$$

For the sake of simplicity, several assumptions are used in this study. First, the unit-cells are assumed to be lossless ($\Gamma_{mn} = 1$) and isotropic ($f(\theta, \phi) = 1$). Furthermore, the metasurfaces are illuminated with normal incidence ($e^{j\alpha_{mn}} = 1$) and unit amplitude ($E_0 = 1$). Therefore, the degrees of freedom for manipulating the reflected EM wave are only the reflection phases φ_{mn} .

Scattered field and autocorrelation

The scattered field E_s can be expressed from a Fourier transform (FT). For the sake of simplicity, let's consider a linear array of N unit-cells with spacing d oriented along the z -direction. Then, equation (1) can be written as (2) with $z = e^{jkd \cos \theta}$ and $a_n = e^{j\varphi_n} = \pm 1$ due to the phase responses of a 1-bit coded metasurface

$$E_s(\theta) = \sum_{n=0}^{N-1} a_n z^n \tag{2}$$

The squared magnitude of the radiated field is written as (3) with $l = n - m$

$$|E_s|^2 = \sum_{n=0}^{N-1} \sum_{m=0}^{N-1} a_{l+m} a_m^* z^l \tag{3}$$

Equation (3) can be rewritten as,

$$|E_s|^2 = \sum_{l=-2N}^{+2N} R_a(l) e^{jlk d \cos(\theta)} \tag{4}$$

where

$$R_a(l) = \sum_{m=0}^{N-1} a_{l+m} a_m^* \tag{5}$$

R_a represents the autocorrelation of the sequence a where the shift l ranges from $-N$ to $+N$. It is well-known the FT of the unit impulse is a constant function. Then, in order to produce a constant

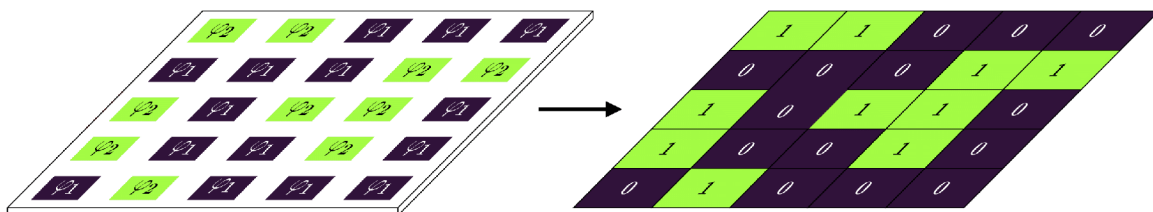


Figure 2. Coding metasurface example.

scattered field (which guarantees a low RCS), the autocorrelation of the used code must resemble the unit impulse as much as possible.

Various families of codes with interesting autocorrelation properties are available in the literature, such as Barker [14] or Golay codes [6]. These codes, originally used in other fields like spread spectrum and radar pulse compression, find their relevance in metasurface coding.

Existing codes

Barker codes are characterized by a main peak $R_a(0) = N$ and secondary peaks $R_a(l)$ for $l \neq 0$ all equal to 0 or -1 . As a result, their autocorrelation function closely approximates a unit impulse function. However, there are only nine different Barker codes and the maximum size is $N = 13$.

Golay codes are other codes that have been used for diffuse scattering metasurfaces due to their good autocorrelation properties. Their main advantage is that they can be defined analytically by (6) using generator polynomials P and Q

$$\left. \begin{aligned} P_0 &= Q_0 = 1 \\ P_{i+1}(x) &= P_i(x) + x^{2^i} Q_i(x) \\ Q_{i+1}(x) &= P_i(x) - x^{2^i} Q_i(x) \end{aligned} \right\} \text{ for } i \geq 0. \quad (6)$$

This analytical derivation process drastically simplifies the generation of these codes. Moreover, contrary to Barker codes, Golay codes do not suffer any stringent size limitation. Indeed, the only constraint is that the produced coding sequence a_n is of size $N = 2^i$ with i an integer number. In practice, this enforces to use a metasurface with a number of unit-cells which is a power of 2. This can be a tricky point regarding the design of the unit-cell since it puts constraints on the inter-element spacing d . Also, despite their good autocorrelation properties, Golay codes are usually not the best possible solutions. They are usually referred to as suboptimal solutions.

MPS codes

Identifying binary codes with optimal or quasi-optimal autocorrelation properties is a research direction that is very active in several domains [14]. These codes are referred to as MPS when the peaks of R_a (except from $R_a(0)$ that is always equal to N) is minimized. Other figures of merit have also been used, such as integrated side-lobe level (ISL) [15], calculated as (7), which gives a global measure of all peaks

$$\text{ISL} = \sum_{l=1}^{N-1} |R_a(l)|^2. \quad (7)$$

This involves summing the squared secondary peaks of the autocorrelation. Since the autocorrelation is always symmetric relative to the main peak, this summation can be performed from $l = 1$ to $l = N - 1$. The derivation of MPS cannot be done analytically. It usually relies on optimization algorithms [15–18] or exhaustive analyses [19] of the autocorrelation function. However, many studies have been carried out and a huge quantity of tabulate data is now available whatever the values of N up to $N = 74$ [19]. In [16], the search has even been extended up to $N = 300$ although the provided codes are not actual MPS but quasi-MPS codes (which means codes with better properties could still be found). In this paper, available databases of MPS codes will be used. An assessment of their properties in the specific context of diffuse scattering

metasurface will be performed. It has never been done from our best knowledges.

To conclude, these codes are interesting in the context of coding diffuse metasurfaces due to their good autocorrelation properties and their approximation to the unit impulse function as well. The link between good autocorrelation properties of codes and the diffusion of the reflected field is verified in the next section through an exhaustive study for small dimension problems.

1D coding metasurfaces for diffuse scattering

Exhaustive search of optimal codes

The goal of this section is to find and analyze the codes that produce the best diffuse radiation and to validate the interest of codes with good autocorrelation properties. In order to make an exhaustive search possible, the canonical case of a 1D metasurface is considered.

To determine the optimal codes, the exhaustive search is conducted by testing all possible coding sequences. That is, for a given size N , the 2^N binary combinations are generated. Then, the scattering field E_s is computed for each configuration and the associated directivity is calculated as (8) [13]

$$D(\theta) = \frac{2 |E_s(\theta)|^2}{\int_0^\pi |E_s(\theta)|^2 \sin \theta d\theta}. \quad (8)$$

Finally, the code with the lowest maximum directivity is identified as the optimal one. This study is done for plane-wave illumination with normal incidence on the 1D metasurface. The interspacing element d is assigned to 0.5λ . The study is conducted for sizes N ranging from 3 to 24 elements. Larger sizes would have resulted in an excessive number of configurations to analyze.

Comparison between available codes

Figure 3 presents the results of this exhaustive search. For each value of N (from 3 to 24), it gives the maximum directivity of few codes. The blue crosses correspond to the worst codes, i.e. the ones with the highest directivity. As could be expected, they are uniform codes (with $a_n = -1$ or $a_n = +1$ whatever n) and they produce a maximum directivity equal to $10 \log(N)$. Therefore, this is the reference case for quantifying the RCSR performance of diffuse scattering codes. On the contrary, the blue circles correspond to the best codes. All other codes, namely the $2^N - 2$ remaining ones, lie within these upper and lower bounds. They are not shown for the sake of clarity.

Barker, Golay, and MPS codes are also included, when they exist, to visualize their performance compared to the optimal ones. Barker codes are the optimal ones except for $N = 13$. Golay codes are not far from the minimum, making them a suboptimal solution except for the length 4 case for which the Golay code is the optimal one and also a Barker code.

MPS codes in black and red dots are selected from [19] and [16] respectively. As mentioned earlier, there can be codes with identical autocorrelation properties for a given size N . However, the resulting directivities may differ but still remain very low. Therefore, the use of MPS codes for coding diffuse scattering metasurfaces represents a new family of suboptimal solutions considering these results.

One strength of these codes is that they are available for any size N , extending beyond 24. It is noteworthy that Barker codes are MPS codes at the sizes for which they exist.

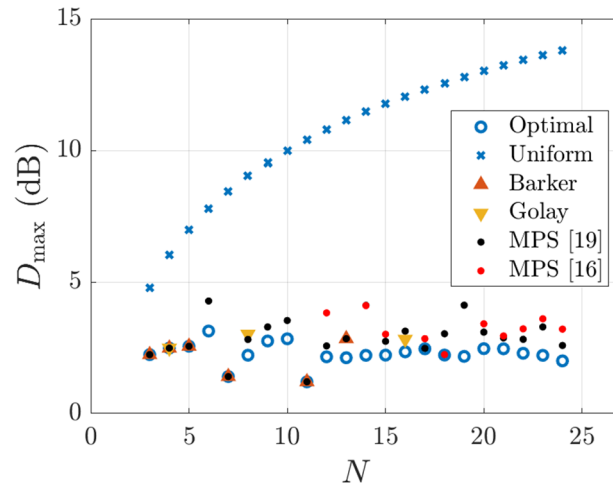


Figure 3. Maximum directivity of different codes for lengths ranging from 3 to 24 elements.

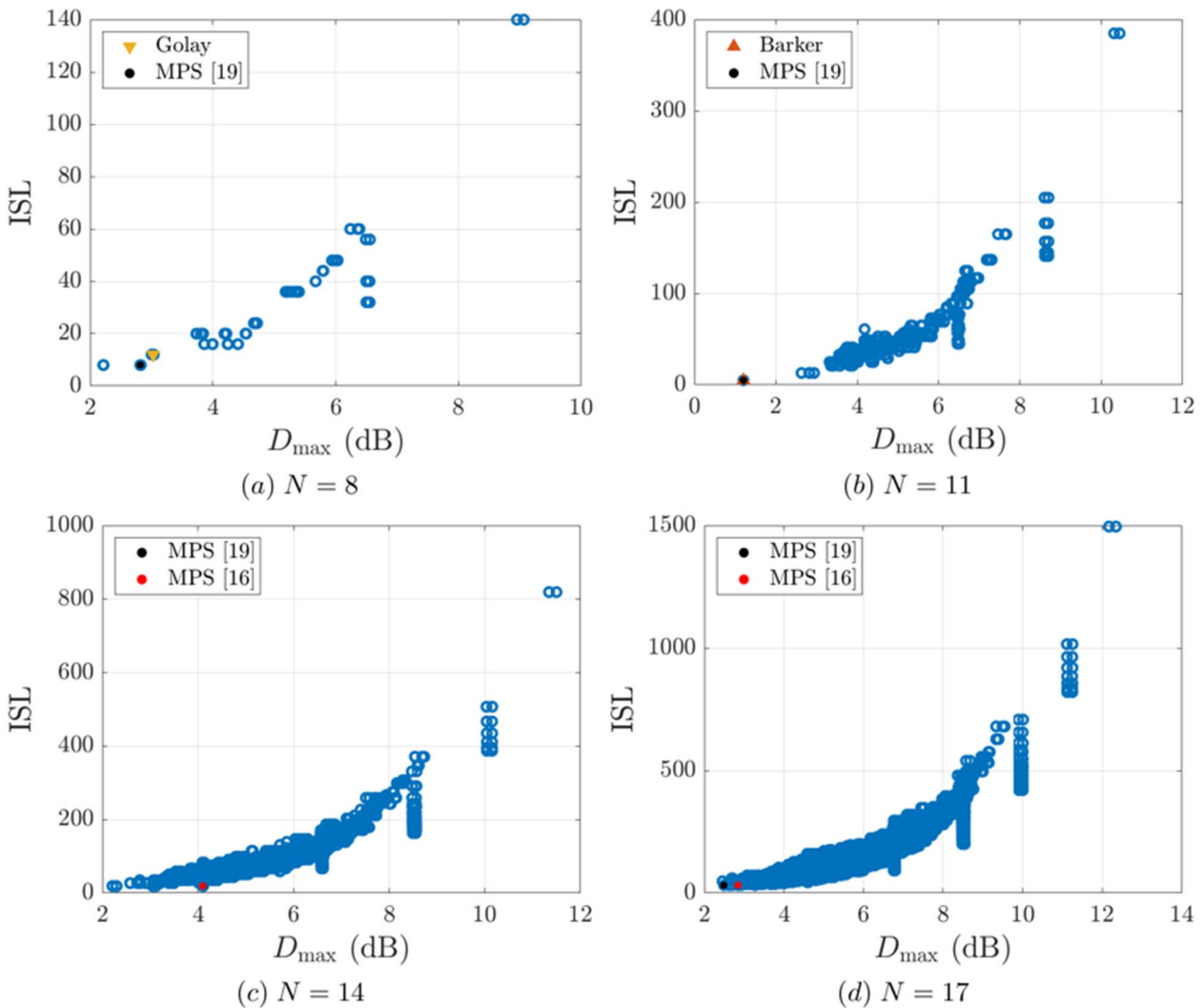


Figure 4. (D_{\max}, ISL) maps of all possible configurations for different given sizes.

Validation of diffuse radiation codes with good autocorrelation properties

To better show the relation between good autocorrelation properties and diffuse radiation, the ISL criteria is now used.

Figure 4 illustrates the complete set of the 2^N codes with their respective maximum directivity and ISL for four different values of N . The optimal code, which exhibits the lowest directivity, is depicted by the blue circle located farthest to the left on these plots. The placement of MPS codes is also specified within the set

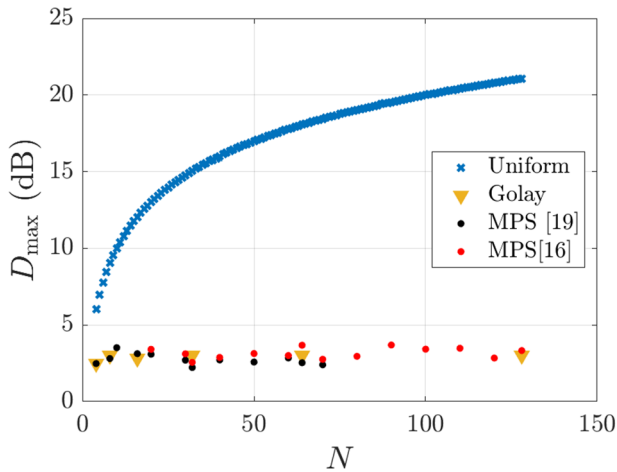


Figure 5. Maximum directivity for Golay and MPS codes with large sizes.

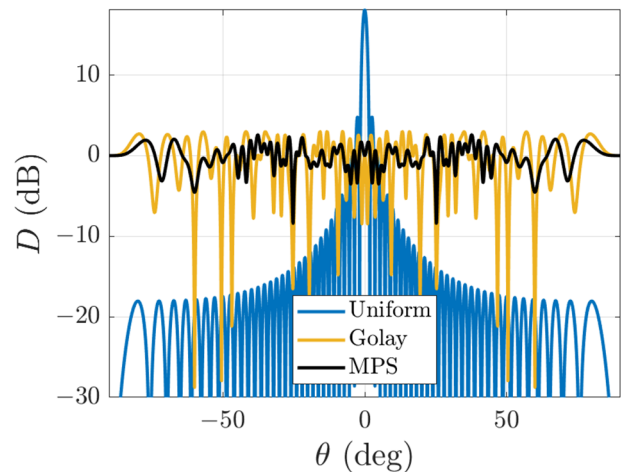


Figure 6. Directivity of uniform, Golay and MPS codes for a 1D metasurface with $N = 64$.

of combinations for each size. Golay and Barker codes are also included for sizes 8 (Figure 4(a)) and 11 (Figure 4(b)) respectively.

From these plots, it is obvious that good autocorrelation properties ensure low directivity. However, codes with the best autocorrelation properties do not necessarily guarantee the lowest directivity. MPS codes are always close to the optimal case. For a given size N , there exists a set of MPS codes as mentioned earlier, the other MPS codes besides those referenced as [19] and [16] can achieve even lower directivity. This is clearly visible in Figure 4(a) with the circle just to the left of the selected MPS code. They share the same ISL but generate different directivities. The situation is identical for $N = 14$ in Figure 4(c). The two chosen MPS codes exhibit nearly identical directivity, making them nearly overlapping on this plot. Other MPS codes of the same size with equally ISL show lower directivity. In the case of $N = 11$ shown in Figure 4(b), unsurprisingly, the Barker code shows the minimum ISL and directivity. Finally, the selected MPS codes of size $N = 17$ are very close to the optimal one as illustrated in Figure 4(d).

Design examples

Directivity of 1D diffuse scattering metasurfaces

The new MPS suboptimal solution can now be compared to the existing one in the literature i.e. by Golay codes. For this purpose, Figure 3 can be extended to longer lengths as shown in Figure 5. On this extended plot, the upper bound stays at $10\log(N)$. The lower bound, which was previously shown for codes ranging from 3 to 24 elements, is omitted here for the sake of clarity. Indeed, an exhaustive search for codes achieving low directivity becomes too expensive in computing resources for sizes larger than 24. Golay codes, available for sizes that are powers of 2, are compared to MPS codes of the same sizes. MPS codes of lengths in tens are included, but it should be noted that they are applicable for any N as mentioned earlier. It can be seen that the performance of MPS codes is very similar to that of Golay ones without suffering their restriction on N .

An example of a directivity pattern is shown in Figure 6. A comparison of the directivities of 1D metasurfaces with 64 elements for different codes is provided. The uniform case, which is the reference to quantify the RCSR, exhibits a maximum directivity of

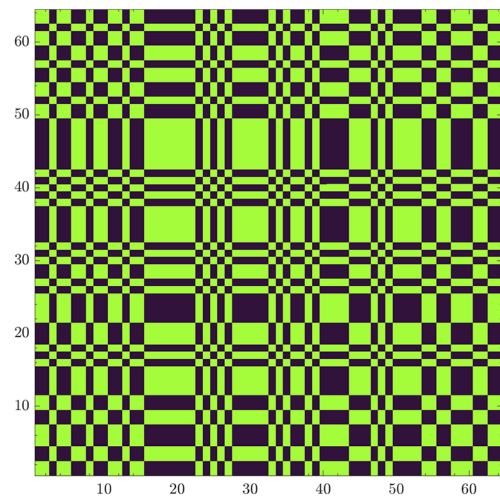


Figure 7. 2D MPS-coded metasurface with 64×64 elements.

18.06 dB. The Golay-coded metasurface has a maximum directivity of 3.00 dB, while the MPS-coded one from [19] has a maximum directivity of 2.58 dB. The performance of the MPS code is superior to the Golay one in this case. These performances can reverse for other lengths in powers of 2. Lower directivities can also be achieved by MPS codes of lengths close to those where Golay can exist as shown in Figure 5.

Extension to 2D diffuse scattering metasurfaces

Previous codes can be extended to 2D metasurfaces using the standard dyadic product [6, 7]. In this case, the same code is assumed for the two directions. This is the most used method in the literature and cost-effective to implement. Using the previous 1D MPS code of length 64, the matrix depicted in Figure 7 can be generated using a dyadic product, with green and black indicating binary elements 1 and 0 respectively. Thus, the outcome yields a matrix comprising 4096 elements. Inter-element spacing d_x and d_y are assigned to 0.5λ .

The reflected field $|E_s|_{dB}$ computed by equation (1) on the metasurface is diffused with low intensity in all directions, as

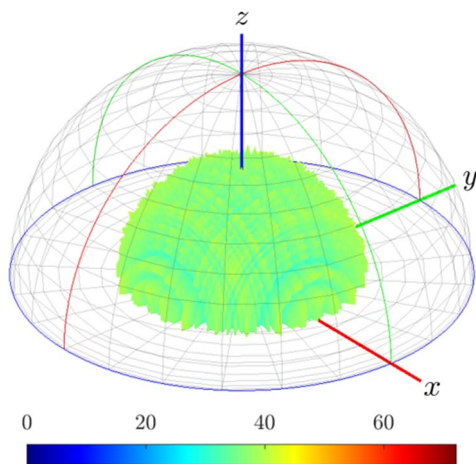


Figure 8. 3D radiation of the 64×64 MPS metasurface.

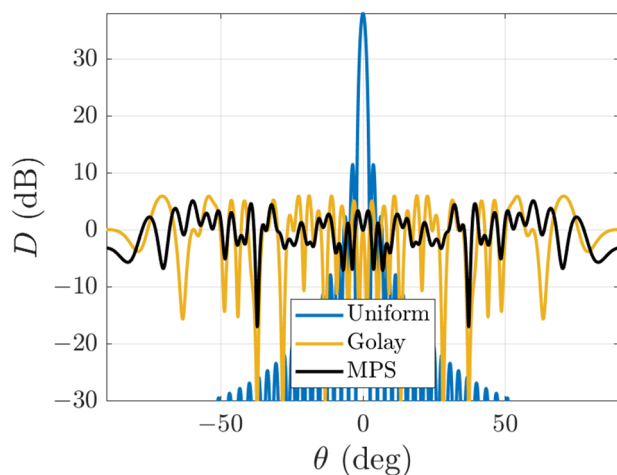


Figure 9. Directivity of uniform, Golay and MPS metasurfaces with size 64×64, $\phi = 45^\circ$.

shown in Figure 8. The associated maximum directivity is 5.16 dB. Directivity in the cut plane $\phi = 45^\circ$, where the maximum is located, is shown in Figure 9. This result is compared to the 2D metasurface of 64×64 elements encoded with Golay code using the dyadic product. This metasurface exhibits a maximum directivity of 6.05 dB.

Conclusion

This paper introduces a new method based on code autocorrelation for encoding diffuse scattering metasurfaces of any size, including large ones. After identifying the optimal codes that achieve the minimum maximum directivity for 1D metasurfaces of small size, the performance of MPS codes is compared to these optimal ones. A strong correlation between good autocorrelation properties and low directivity is demonstrated using the ISL metric. Additionally, calculating the autocorrelation is much less computationally expensive than calculating the backscattered field E_s and the directivity. This approach offers new possibilities by focusing on the autocorrelation of the codes instead of optimizing the coding matrix to diffuse the incident EM wave and thus to decrease the RCS. As the method is evaluated using analytical modeling, future

work will focus on experimental validations. In particular, the predicted RCS of MPS codes will be verified through EM simulations and measurements.

Acknowledgements. This work is funded by the French organizations Centre National des Études Spatiales (CNES) and Agence Innovation Défense (AID).

Competing interests. None.

References

- Díaz-Rubio A, Asadchy VS, Elsakka A and Tretyakov SA (2017) From the generalized reflection law to the realization of perfect anomalous reflectors. *Science Advances* 3(8), e1602714.
- Sun S, He Q, Xiao S, Xu Q, Li X and Zhou L (2012) Gradient-index metasurfaces as a bridge linking propagating waves and surface waves. *Nature Materials* 11(5), 426–431.
- Lipuma D, Méric S and Gillard R (2013) RCS enhancement of flattened dihedral corner reflector using reflectarray approach. *Electronics Letters* 49(2), 152–154.
- Paquay M, Iriarte J-C, Ederra I, Gonzalo R and de Maagt P (2007) Thin AMC structure for radar cross-section reduction. *IEEE Transactions on Antennas and Propagation* 55(12), 3630–3638.
- Chen W, Balanis CA and Birtcher CR (2015) Checkerboard EBG surfaces for wideband radar cross section reduction. *IEEE Transactions on Antennas and Propagation* 63(6), 2636–2645.
- Moccia M, Liu S, Wu RY, Castaldi G, Andreone A, Cui TJ and Galdi V (2017) Coding metasurfaces for diffuse scattering: Scaling laws, bounds, and suboptimal design. *Advanced Optical Materials* 5(19), 1700455.
- Cui TJ, Qi MQ, Wan X, Zhao J and Cheng Q (2014) Coding metamaterials, digital metamaterials and programmable metamaterials. *Light: Science & Applications* 3(10), e218.
- Yang H, Cao X, Yang F, Gao J, Xu S, Li M, Chen X, Zhao Y, Zheng Y and Li S (2016) A programmable metasurface with dynamic polarization, scattering and focusing control. *Scientific Reports* 6(1), 35692.
- Su P, Zhao Y, Jia S, Shi W and Wang H (2016) An ultra-wideband and polarization-independent metasurface for RCS reduction. *Scientific Reports* 6(1), 20387.
- Xu Y, Liu J, Gao L, Ai X, Zhang Z and Liang H (2022) 1-bit coding metasurface for wideband RCS reduction. In *2022 International Applied Computational Electromagnetics Society Symposium (ACES-China)*, Xuzhou, pp. 1–3.
- Liu X, Gao J, Xu L, Cao X, Zhao Y and Li S (2017) A coding diffuse metasurface for RCS reduction. *IEEE Antennas and Wireless Propagation Letters* 16(1), 724–727.
- Zhao Y, Cao X, Gao J, Sun Y, Yang H, Liu X, Zhou Y, Han T and Chen W (2016) Broadband diffusion metasurface based on a single anisotropic element and optimized by the simulated annealing algorithm. *Scientific Reports* 6(1), 23896.
- Balanis CA (2016) *Antenna Theory: Analysis and Design*, 4th Edn.
- Golomb S and Gong G (2005) *Signal Design for Good Correlation: For Wireless Communication, Cryptography, and Radar*.
- Song J, Babu P and Palomar DP (2015) Optimization methods for designing sequences with low autocorrelation sidelobes. *IEEE Transactions on Signal Processing* 63(15), 3998–4009.
- Dimitrov M, Baicheva T and Nikolov N (2021) Hybrid constructions of binary sequences with low autocorrelation sidelobes. *IEEE Access* 9(1), 112400–112410.
- Tang L, Zhu Y and Fu Q (2018) Fast algorithm for designing periodic/ap-periodic sequences with good correlation and stopband properties. *EURASIP Journal on Advances in Signal Processing* 2018(1), 57.
- Lin R, Soltanalian M, Tang B and Li J (2019) Efficient design of binary sequences with low autocorrelation sidelobes. *IEEE Transactions on Signal Processing* 67(24), 6397–6410.

19. **Leukhin AN and Potekhin EN** (2013) Optimal peak sidelobe level sequences up to length 74. In *2013 European Microwave Conference*, Nuremberg, pp. 1807–1810.



Thomas Uguen is currently pursuing his Ph.D. at the National Institute of Applied Sciences (INSA) of Rennes, France. His research focuses on the use of metasurfaces for radar applications and is conducted in collaboration with the Institut d'Électronique et des Technologies du numérique (IETR) and the Centre National des Études Spatiales (CNES).



Raphaël Gillard was born in France in 1966. He received the Ph.D. degree in electronics from INSA Rennes, France, in 1992. He was first a Research Engineer within IPSIS Company before joining INSA again. Since 2001, he has been a Full Professor within the “Institut d'Électronique et des Technologies du numérique” (IETR) in Rennes. From 2006 to 2020, he was co-leading the Antenna and Microwaves Department of IETR. From 2015 to 2020, he was the academic chair of the MERLIN Laboratory, a joint laboratory between IETR and Thales Alenia Space. His main research interests include antenna arrays, reflectarrays, and periodic structures. He is teaching electromagnetics, microwaves, and antennas. He is in charge of a Master Program and is participating in the European School of Antenna (ESoA).



Renaud Loison is professor at the Institut National des Sciences Appliquées (INSA), Rennes, France. He carries out his research activity at the Institut d'Électronique et des Technologies du numérique (IETR) and mainly works on antenna measurement, reflectarrays, metasurfaces, and more generally on periodic and quasi-periodic surfaces.



Jeanne Pagés-Mounic received the bachelor's degree in electronics, electrical energy and automation (EEA) from the Jean-François Champollion University Center, Albi, in 2016, and the master's degree in electronics, embedded systems, and telecommunications (ESET) from Paul Sabatier University, Toulouse, in 2018. She received her Ph.D. degree completed at ONERA Toulouse in the field of space antennas, particularly in transmit-arrays, in December 2021. Immediately afterward, she was hired by CNES in the Antennas department, in which she has worked ever since.



Philippe Pouliguen received the M.S. degree in signal processing and telecommunications, the Doctoral degree in electronic and the “Habilitation à Diriger des Recherches” degree from the University of Rennes 1, France, in 1986, 1990 and 2000. In 1990, he joined the Direction Générale de l'Armement (DGA) at the Centre d'Électronique de l'Armement (CELAR), now DGA Information Superiority (DGA/IS), in Bruz, France, where he was a “DGA senior expert” in electromagnetic radiation and radar signatures. He was also in charge of the EMC (Expertise and ElectroMagnetism Computation) laboratory of DGA/IS. From 2009 to 2018, Dr. Pouliguen was the head of “acoustic and radio-electric waves” scientific domain at DGA, Paris, France. Since 2018, he is Innovation Manager of the “acoustic and radio-electric waves” domain at the Agence Innovation Défense (AID). His research interests include electromagnetic scattering and diffraction, radar cross-section (RCS) measurement and modeling, asymptotic high frequency methods, radar signal processing and analysis, antenna radiation and scattering problems, metamaterials, and metasurfaces.